Evidence for hetero-association of transmembrane helices of integrins

Kay-Eberhard Gottschalk[a], Horst Kessler[b,*]

[a] Department of Biological Chemistry, Weizmann Institute of Science, Herzl St 1, 76100 Rehovot, Israel
[b] Institut fuer organische Chemie und Biochemie, Technische Universitaet Muenchen, Lichtenbergstr. 4, 85747 Garching, Germany

Received 10 October 2003; revised 10 October 2003; accepted 6 November 2003

First published online 29 December 2003

Edited by Thomas L. James

Abstract **Integrins are important transmembrane cell-surface receptors, which mediate interactions of the cell with other cells or the extracellular matrix. Integrins are heterodimers composed of an α- and a β-subunit. They can switch between different activation states depending on intra- or extracellular signals. Inside/out and outside/in signaling is mediated via integrins across the membrane. A biologically important and yet still unanswered question is the role of the transmembrane domains in the signaling event. Here it is shown by simulated annealing/molecular dynamics calculations that recently published structural data of the cytoplasmic domains of integrin αIIbβ3 are supporting a structure with interacting transmembrane helices. This corroborates a model of transmembrane domains that are actively involved in the transmembrane signaling event.**

Key words: Integrin; Signaling; Nuclear magnetic resonance structure; Molecular dynamics; Helix interaction; Transmembrane

1. Introduction

In each cellular organism information has to be passed through cellular membranes in order to allow cells to communicate with other cells or the extracellular matrix. In general, transmembrane receptors or ion channels transmit signals or matter through the membrane in order to fulfill this task. An important class of transmembrane receptors is the class of integrins [1].

Integrins are involved in a large number of fundamental cellular processes like cell-matrix adhesion, differentiation, proliferation, apoptosis and stress response [2]. They are composed of two subunits, α and β, each featuring a large extracellular domain, a single membrane spanning helix and a short cytoplasmic domain [3]. Crystallographic studies of the extracellular domain have vastly increased our understanding of ligand binding and specificity [4,5]. Recently, nuclear magnetic resonance (NMR) studies tried to determine the structure of the intracellular domains of the αIIbβ3 integrin [6–8].

While some biochemical and structural studies indicate a tendency of the transmembrane domains of integrins to interact as heterodimers [9,10], other studies did not find these interactions [11,12]. The answer to the question whether the transmembrane domains of integrin complexes are actively involved in the signaling event (and thus interact with each other, putatively fine-tuning the structural changes involved in signaling as suggested previously) or just serve as a mechanical junction between the intracellular and extracellular domains is of major importance for the understanding of signaling [13].

Due to the shortness of the biochemical construct used for a recently published NMR structure of the cytoplasmic domain of αIIbβ3 (pdb code 1M8O.pdb) [8], it cannot be deduced from the structure whether the measured intersubunit NOEs are in accordance with a integrin model of interacting transmembrane domains. On the contrary, it has been suggested that these data are contradictory to such a model [12]. Furthermore, the NOE restraints obtained from the NMR measurements are at the N-terminal end of a short helix in the reported structure. It is well known that the termini of helices are rather flexible and tend to fray [14–16], possibly affecting the validity of the published structure.

We therefore decided to recalculate the structure in the context of an extended construct, which in a first step entails seven additional N-terminal residues and forces the residues corresponding to residues 1–9 of the α-subunit as well as the entire β-subunit of 1M8O to adopt a helical conformation. In a second step we further prolonged the helices with another seven N-terminal residues per helix. For our calculations we truncated the β-subunit at residue 35 of 1M8O. It can be safely assumed that the α- and β-subunit are continuously helical from the membrane into the cytoplasmic, membrane proximal space [3,9,13]. The added N-terminal (membrane proximal) residues comprise thus two respectively four helical turns. The extension serves the purpose to minimize structural deviations at the site where intersubunit NOEs have been observed. The sequence of the original construct and the additions are shown in Fig. 1 together with the location of the NOE restraints.

We will show that in the context of our model construct the available data support a model of interacting transmembrane helices. We will furthermore argue that this model is most probably the physiologically important one.

2. Materials and methods

All the calculations have been performed using CNS, vers. 1.1 [17]. Starting from an extended random structures with αIIb and β3 being oriented parallel to each other with the N-termini pointing to the same direction, two different simulated annealing/molecular dynamics schemes were performed in different steps. The one simulation forced the helical parts to be strictly α-helical, while in a second run also 3(10)- or pi-helices were allowed. The first calculation was performed as follows: first, a high-temperature torsion angle molecular dynamics

*Corresponding author. Fax: (49)-89-289 13210.
E-mail address: horst.kessler@ch.tum.de (H. Kessler).

0014-5793/03/$30.00
doi:10.1016/S0014-5793(03)01443-1

calculation at 50 000 K with 1000 steps and a time step of 15 fs was performed. The scale factor for the vdw term was 0.01, for the NOE term 150 and for the dihedral restraint term 25. This was followed by a torsion angle dynamics cooling stage in which the system was cooled from 50 000 K to 0 K with 1000 steps, a time step of 15 fs and a temperature step of 250 K. This means that the system was simulated at 200 decreasing temperatures, with five time steps per temperature. The scale factor for the vdw term was increased from 0.01 to 1 during this stage. The NOE term scale factor was kept at 150, the dihedral angle restraint term was scaled with a factor of 200. A cooling stage with Cartesian dynamics followed, cooling the system from 1000 K to 0 K with 1000 steps, a time step of 5 fs and a temperature step of 25 K. Here the system was simulated at 40 decreasing temperatures, with 25 time steps per temperature. During this second cooling stage the vdw scale factor was increased from 1 to 4, the NOE term was scaled with a scale factor of 450 and the dihedral term with a factor of 200. Ten cycles of Powell minimization with 200 steps per cycle followed. During the minimization the NOE term was scaled with a factor of 75 and the dihedral term with a factor of 400. The following restraints were used during all steps: (a) dihedral restraints for the phi and psi angles of the helical parts of the backbone and NOE-like hydrogen-bonding restraints with 3.1 Å between N_i and O_{i+4} and 2.1 Å between H_i and O_{i+4} for the helical parts of the model; (b) NOE-like restraints for the non-helical C-terminus of the α-subdomain to ensure a conformation similar to the published conformation of the C-terminus; (c) all 11 intersubunit restraints determined by Vinogradova et al. [8]. For further calculations additional restraints have been introduced: a biochemically determined intersubunit salt-bridge restraint and in a final run helix–helix center restraints, which restrain the centers of the N-termini of the helices to be closer than 12 Å (Fig. 1).

The second calculation, which allowed the occurrence of 3(10)- and π-helices, followed the same scheme, but with different scaling factors for the dihedral term and different NOE restraints. The dihedral term had a scaling factor of 25 for the high-temperature step, a scaling factor of 75 for the first and the second slow-cool annealing stage and a scaling factor of 25 for the final minimization stage. Ambiguous NOE restraints with R-6 averaging were used with 3.1 Å between N_i and O_{i+3} or O_{i+4} or O_{i+5} and with ambiguous restraints of 2.1 Å between H_i and O_{i+3} or O_{i+4} or O_{i+5} for the helical parts of the model. While the first calculation is optimized for good convergence to an α-helical structure, the second calculation allows a higher flexibility, but still prefers an α-helical structure where possible.

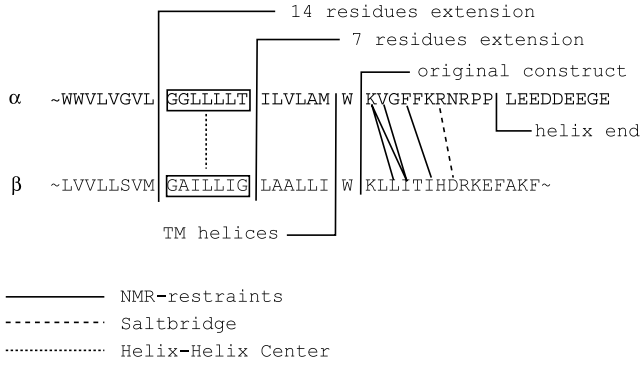

Fig. 1. Sequence of α- and β-subunit: Starting with the transmembrane domain, the sequence of the α- and β-subunit is shown together with the parts used in the presented work and in the original construct. The position of the different used interdomain restraints has been indicated by lines connecting the respective amino acids. The center of mass of the first seven residues of each subunit has been restrained to be closer than 12 Å in the final calculation with 14 additional residues. Both subunits have large extracellular domains. The β-subunit has additional C-terminal amino acids.

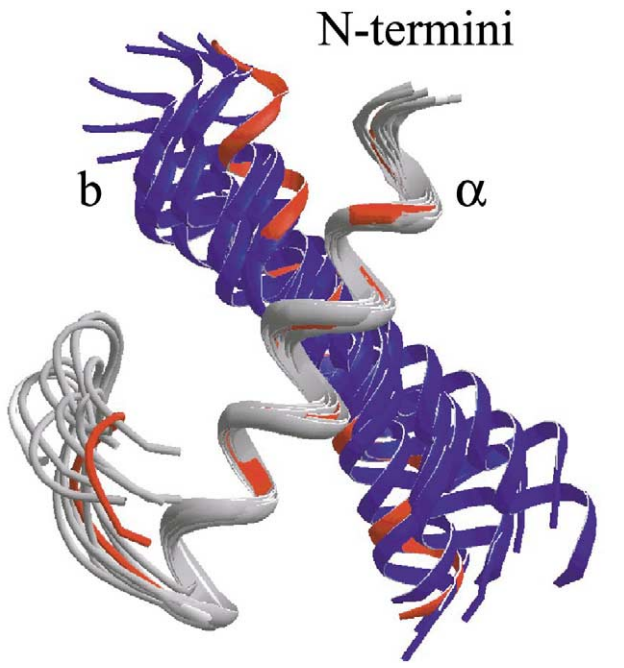

Fig. 2. Crossing angles of 10 low-energy structures with end-on salt-bridge: After superposition of the helical part of the α-domain (in front), it can be seen that despite the reasonable convergence of the calculation the crossing angle between the helices is ill-defined by the 11 intersubunit NOE restraints. All of the shown structures do not violate any intersubunit restraint. The lowest-energy structure (red) has a crossing angle that is compatible with interacting transmembrane domains. The figure is generated with SwissPdbViewer. (For interpretation of the references to color in this figure legend, the reader is referred to the web version of this article.)

3. Results and discussion

3.1. Calculation I

To investigate the possibility of the measured restraints to determine the structure of the cytoplasmic domain in an extended helical model, we performed 100 simulated annealing/molecular dynamics calculations of the peptide N-terminally extended by seven wild-type residues of the integrin sequence (Fig. 1), using the intersubunit NOE data of the original publication by Vinogradova et al. [8] as described in Section 2. The original 11 intersubunit NOE restraints were kindly provided by Vinogradova and Qin. Our calculations demonstrate that in the context of our extended helical construct all restraints can be fulfilled. Albeit, the 10 lowest-energy structures do not only not converge, but also most of the structures display an orientation of the two subunits, in which the N-termini of both subunits point in opposite directions. Since the N-termini of the subunits are extensions of the transmembrane domains of the subunits, they both have to point towards the membrane and thus into the same direction. The predominantly obtained orientation is therefore incorrect.

The average RMSD to the mean structure of the 10 lowest-energy structures is 3.3 Å. The lack of convergence and the predominantly incorrect orientation demonstrates that the measured restraints are not sufficient to unambiguously define the structure of the cytoplasmic domain of αIIbβ3 integrin in a meaningful way. As even the strict α-helical simulation scheme did not lead to convergence of the structures, the more flexible scheme has not been applied.

3.2. Calculation II

In order to further restrain the system, we included a biochemically determined salt-bridge [18] as a restraint in the SA/MD calculations (see Fig. 1). The salt-bridge was included either as a side-on or as an end-on salt-bridge between the residues corresponding to Arg 7 and Asp 28 of 1M8O. Both salt-bridge types were calculated together with the original set of NOE restraints. Including the salt-bridge improves the convergence significantly: the average RMSD of the Cα-atoms to the mean structure of the 10 lowest-energy structures is only 1.5 Å for the end-on salt-bridge (one additional restraint) and 1.3 Å for the side-on salt-bridge (two additional restraints), when using the strict α-helical restraints. Furthermore, the structures now adopt a biologically sensible head-to-head orientation. Despite the reasonable convergence, the crossing angle between the helices is still not well defined (Fig. 2). While the lowest-energy structure of the ensemble with the end-on salt-bridge (red in Fig. 2) has a crossing angle of 24.5° relative to the central axis between the helices, compatible with an interaction of the transmembrane helices, other structures with higher crossing angles exist in the ensemble of the 10 lowest-energy structures. The average crossing angle is $31.9 \pm 5.5°$ for the ensemble with end-on salt-bridge and $29.8 \pm 4.5°$ for the ensemble with side-on salt-bridge, indicating rather large fluctuations of the crossing angles of the structures in the ensemble. The RMSD between the backbones of the averaged structures of both calculations (with end-on and with side-on salt-bridge) is 0.8 Å, indicating that the choice of the salt-bridge is of minor importance. The possibility to include the biochemically determined salt-bridge without violating the measured NOEs gives confidence in the biological relevance of the construct used and the contacts measured by Vinogradova et al.

Loosening the strictly α-helical restraints and allowing the occurrence of 3(10)- or π-helices reduces the convergence. While the rotational orientation still remains approximately the same, the tilt is even less defined than before. While with strictly α-helical restraints only right-handed tilt angles between the helices are observed, now also left-handed tilt angles are found in the ensemble of low-energy structures.

3.3. Calculation III

As an additional test of the compatibility of the published NMR data with a model of interacting transmembrane domains we further extended the helices N-terminally by another two helical turns (seven residues) of the wild-type sequence, which we forced to interact by restraining the distance between the centers of the two N-terminal helical turns to be less than 12.0 Å. This construct entails approximately half of the predicted transmembrane domains of αIIb and β3, thus providing a good estimate whether or not a model with interacting transmembrane domains is compatible with the measured NOE data. The length of the construct (14 residues per subunit more than in the original construct used by Vinogradova et al., see Fig. 1) in combination with the low number of intersubunit restraints prevents a good convergence of the calculation: the average Cα-RMSD of the 10 lowest-energy structures to the mean structure is 2.4 Å for the end-on salt-bridge and 2.3 Å for the side-on salt-bridge. The convergence increases dramatically when excluding outliers from the ensemble: two structures of the end-on calculation and one structure from the side-on calculation have significantly higher RMSDs to the mean structure than the other structures. Removing these structures and regarding just the helical parts increases the convergence to a Cα-RMSD of 1.4 Å for the end-on calculation and 1.7 Å for the side-on calculation. The existence of the outliers underlines that the system is underdetermined by the used NOEs. Nevertheless, the good convergence of the structures excluding the outliers demonstrates that even with the very limited number of NOEs a reasonable structure including large parts of the transmembrane domains can be calculated. The Cα-RMSD between the helical parts of the averaged structures of the side-on and of the end-on calculation is 1.3 Å. Both structures display a coiled-coil arrangement of the helices extending from the transmembrane domain into the cytoplasmic space (Fig. 3).

Using the relaxed set of helical NOEs hardly changes the outcome of the calculation: the convergence for the end-on salt-bridge is 2.3 Å and for the side-on salt-bridge 2.5 Å with no significant change in the relative orientation between the strict and the relaxed calculation.

The calculated structures show a right-handed coiled-coil structure of helices with an interface similar to that described for 1M8O.pdb. While the C-terminal end of the interface is characterized by electrostatic interactions between the salt-bridge-forming residues, the remaining interface is very hydro-

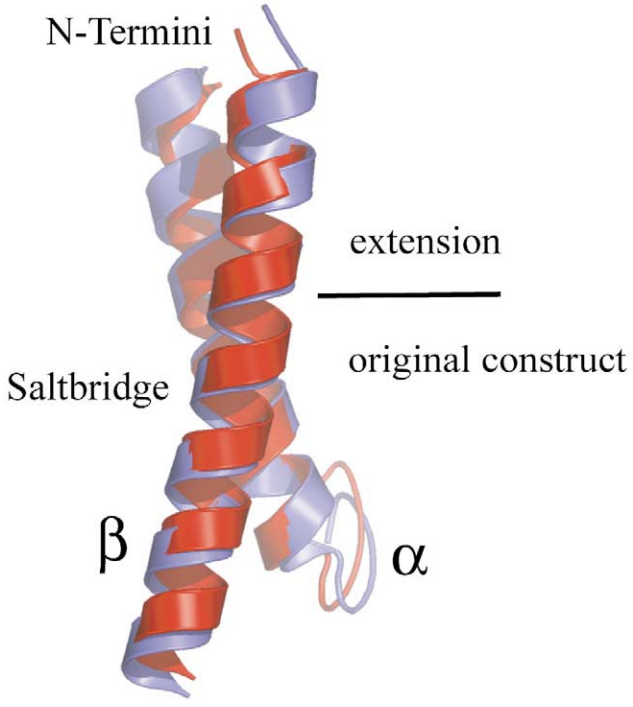

Fig. 3. Possible coiled-coil structure of αIIb-β3. The results of calculation III are shown. The averaged low-energy structures with an end-on (blue) and side-on (red) salt-bridge are drawn as a cartoon representation. The approximate positions of the additional restraints as well as the size of the original construct are depicted. Both structures are virtually identical, with an RMSD of 1.3 Å between the Cα-atoms of the helical parts of both models. The α- and β-subunits interact at the N-termini in the putatively transmembrane region and all intersubunit restraints are fulfilled. This demonstrates that the structural data are in accordance with a model of interacting transmembrane helices. The figure is generated with Pymol (www.pymol.org). (For interpretation of the references to color in this figure legend, the reader is referred to the web version of this article.)

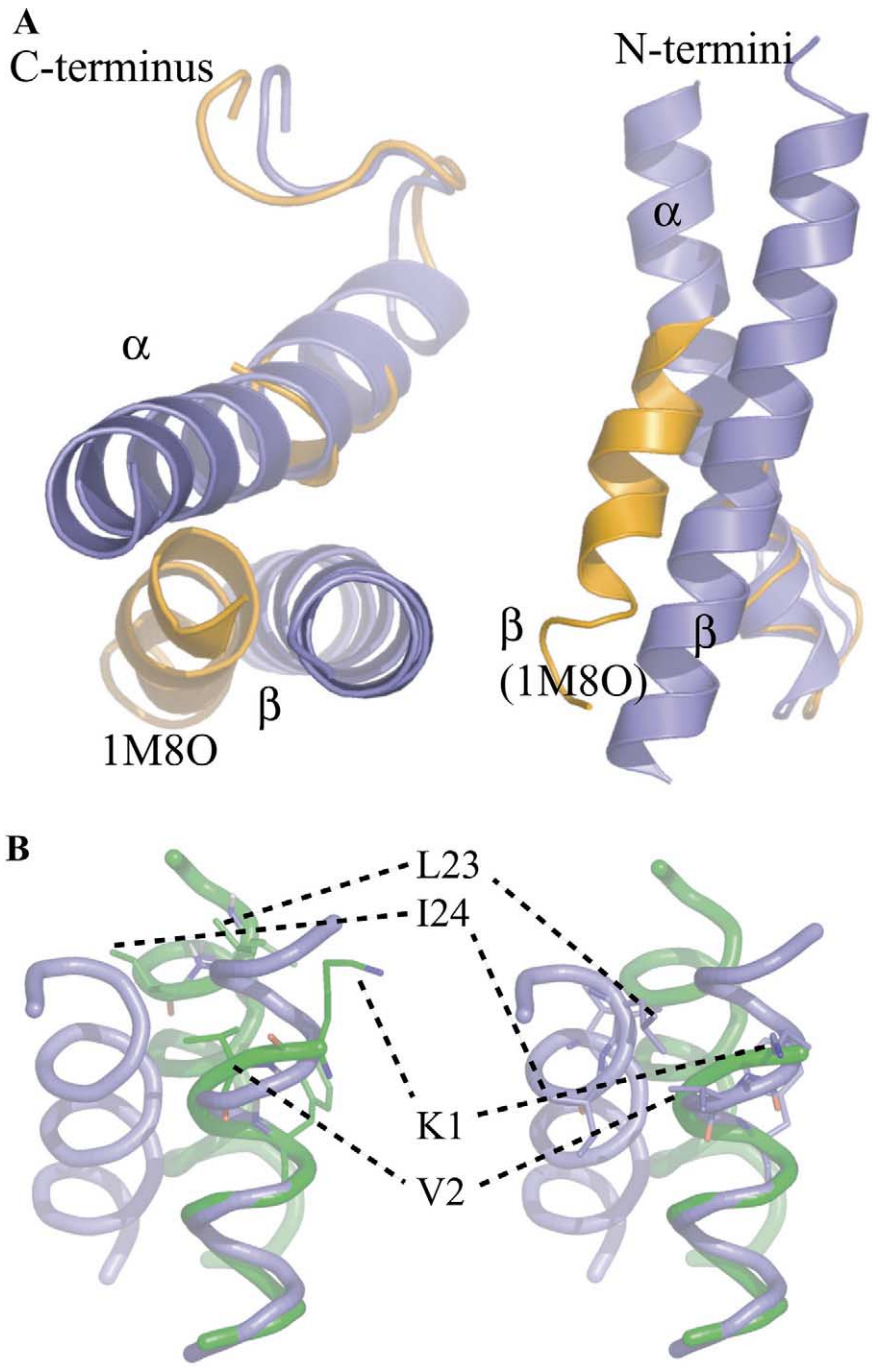

Fig. 4. Comparison of 1M8O with our results. A: Superposition of the helical parts of the α-subunits of our model (blue; average of low-energy structures with end-on salt-bridge, excluding outliers) and 1M8O (orange) reveals differences in the relative orientation of the subunits. These differences are necessary to (a) render the structures compatible with a helical model and (b) to avoid clashes between the prolonged helices of the subunits. *Left*, top view; *right*, side view. B: The residues with NOE restraints are shown after superposition of the helical parts of the α-subunit. Nine of the 11 intersubunit NOEs are measured between K1 and V2 on the α-subunit and L23 and I24 on the β-subunit. While these two residues are not in accordance with a helical model for 1M8O (green, *left*) but either clash with an extended helix (K1) or are in a disallowed region of the Ramachandran plot (V2), both residues are forced to be in the context of a helical structure (blue, *right*). This positions the β-subunit differently. The residue numbering relates to 1M8O.pdb. For 1M8O, model 1 is shown, for our structure, the representative model of the 10 low-energy models is shown. (For interpretation of the references to color in this figure legend, the reader is referred to the web version of this article.)

phobic with no charged contributions. The hydrophobic interface is rich in isoleucine and alanine – both residues that have a restricted mobility already in the monomer and therefore minimize the entropic cost of dimerization. The important role of beta-branched and small residues at right-handed helix–helix interfaces has been recognized before [19,20]. The low number of experimental restraints used here precludes a detailed discussion of the structure and the interface, as the presented calculations are of low resolution. They nevertheless can still prove the main point of our results, namely that the

existing structural data support a model of interacting transmembrane domains for integrins.

Calculation III clearly indicates that the measured NOEs are compatible with a model of interacting transmembrane domains. Excluding outliers of the ensemble of low-energy structures leads to a good (end-on) to reasonable (side-on) convergence of the system. A reasonable structural model of half of the transmembrane domain together with the cytoplasmic domain can be obtained using the NOEs measured by Vinogradova et al.

3.4. Comparison to 1M8O.pdb

While the first 10 models of 1M8O.pdb have an average RMSD of 1.4 Å to the mean structure (when truncating the β3 subunit after residue 35), we cannot reach this convergence without using the biochemically determined salt-bridge as restraint. The main difference in the calculations reported here and the calculations that led to the published NMR structure (apart from the added residues and artificial helical restraints in our calculations, which are two factors that diminish flexibility and reduce the possible set of sidechain conformations and therefore should increase convergence) is the choice of the start structure. While we used an extended conformation as a start structure, which was only biased due to the fact that we positioned the two unstructured subunits parallel to each other with the N-termini pointing to the same direction, Vinogradova et al. first calculated the structures of the subunits independently and in a second step formed the complex from the prefolded subunits. The latter technique probably leads to a significantly improved convergence, but bears the risk of bias: the outcome will be dependent on the initial positioning of the prefolded subunits. The good convergence observed by Vinogradova et al. as opposed to our results reported here might therefore stem from the initial bias introduced by the intuitive choice of the start structure.

Comparing the average structure of the lowest-energy structures of calculation III (with end-on salt-bridge restraint, excluding the two outliers) with the average of the first 10 models of 1M8O.pdb reveals certain differences in the two structures (Fig. 4). The deviations manifest themselves in two ways: (a) the helical parts are strictly helical in our model but show significant deviations from ideal helicity in the NMR structure, which is probably caused by a lack of suitable restraints and the inherent flexibility of the construct used in the work of Vinogradova et al., and (b) by a different relative orientation of the two subunits. The superposition of the helices of the α-subunits of our calculation with 1M8O reveals that an N-terminally extended β-subunit helix of 1M8O would clash with an N-terminally extended α-subunit helix (Fig. 4A).

Two of the three residues in the αIIb subunit of the published NMR structure (1M8O.pdb) involved in NOE contacts with the β-subunit are not compatible with a helical model: the phi-psi angle combination of Val 2 of the representative model (model 1) of 1M8O is in an disallowed region of the Ramachandran plot and Lys 1 of 1M8O displays a sidechain conformation which would clash with an N-terminally extended helix (Fig. 4B). The difference in orientation between the structure reported here and 1M8O might be caused by the fact that both the sidechain conformation of the residue corresponding to Lys 1 in 1M8O and the backbone conformation of the residue corresponding to Val 2 in 1M8O are forced to be in accordance with a helical secondary structure of this part in our model (Fig. 4B), but are more flexible in the calculations of Vinogradova et al. Furthermore, the β-subunit has to adopt a different orientation in our calculation in order to prevent clashes with the longer helix of the α-subunit (Fig. 4A).

From our calculations we can conclude that the reported intersubunit NOEs are in agreement with a helical model of the cytosolic and transmembrane domain of the αIIbβ3 integrin. They support the notion that the transmembrane helices of the integrins interact at least in the low-affinity conformation in a coiled-coil fashion. A model of interacting transmembrane domains is supported by recent biochemical investigations which detect transmembrane interactions using the novel GALLEX system [10]. Furthermore, three-dimensional reconstructions of electron microscopy studies of the full integrin clearly evidence the association of the transmembrane helices [9]. Apparently the interactions between the transmembrane domains seem to be weak, as the GALLEX signal is rather small and other techniques fail to detect any hetero-interactions [11]. Nevertheless, these interactions may be an important contributor to the specificity of integrin dimerization and might fine-tune the signaling.

The presented calculations are in line with experimental biochemical and spectroscopic data that indicate a hetero-dimerization of the transmembrane domains of the integrin αIIbβ3 in the low-affinity state. The sequential, functional and structural relationship between the members of the integrin family renders it probable that this phenomenon is common among the integrins. To our knowledge, the evidence for interacting transmembrane domains in the high-affinity state is weaker than for the low-affinity state. Nevertheless, it seems reasonable to assume that these interactions exist. A separation of the helices in the membrane upon activation would be energetically costly and due to the viscosity of the membrane a slow process. A signaling event involving a conformational change in the sense of a scissors-like movement as suggested earlier by us [21] could gain from potentially increasing interactions between the helices and would be faster, as less work against the membrane lipids would have to be performed. Such a model is in agreement with all biochemical data available. We therefore assume that the transmembrane domains of integrins play an active role in signaling and serve as an additional fine-tuning element in the signaling event.

References

[1] Hynes, R.O. (2002) Cell 110, 673–687.
[2] Buckley, C.D., Rainger, G.E., Bradfield, P.F., Nash, G.B. and Simmons, D.L. (1998) Mol. Membr. Biol. 15, 167–176.
[3] Humphries, M.J., McEwan, P.A., Barton, S.J., Buckley, P.A., Bella, J. and Paul Mould, A. (2003) Trends Biochem. Sci. 28, 313–320.
[4] Xiong, J.P., Stehle, T., Zhang, R., Joachimiak, A., Frech, M., Goodman, S.L. and Arnaout, M.A. (2002) Science 296, 151–155.
[5] Xiong, J.P. et al. (2001) Science 294, 339–345.
[6] Weljie, A.M., Hwang, P.M. and Vogel, H.J. (2002) Proc. Natl. Acad. Sci. USA 99, 5878–5883.
[7] Vinogradova, O., Haas, T., Plow, E.F. and Qin, J. (2000) Proc. Natl. Acad. Sci. USA 97, 1450–1455.
[8] Vinogradova, O., Velyvis, A., Velyviene, A., Hu, B., Haas, T., Plow, E. and Qin, J. (2002) Cell 110, 587–597.
[9] Adair, B.D. and Yeager, M. (2002) Proc. Natl. Acad. Sci. USA 99, 14059–14064.
[10] Schneider, D. and Engelman, D.M. (2003) J. Biol. Chem. 278, 3105–3111.

[11] Li, R., Babu, C.R., Lear, J.D., Wand, A.J., Bennett, J.S. and DeGrado, W.F. (2001) Proc. Natl. Acad. Sci. USA 98, 12462–12467.
[12] Li, R. et al. (2003) Science 300, 795–798.
[13] Liddington, R.C. and Ginsberg, M.H. (2002) J. Cell Biol. 158, 833–839.
[14] Kurutz, J.W. and Lee, K.Y. (2002) Biochemistry 41, 9627–9636.
[15] Neidigh, J.W., Fesinmeyer, R.M., Prickett, K.S. and Andersen, N.H. (2001) Biochemistry 40, 13188–13200.
[16] Luisi, D.L., Wu, W.J. and Raleigh, D.P. (1999) J. Mol. Biol. 287, 395–407.
[17] Brunger, A.T. et al. (1998) Acta Crystallogr. D: Biol. Crystallogr. 54, 905–921.
[18] Hughes, P.E., Diaz-Gonzalez, F., Leong, L., Wu, C., McDonald, J.A., Shattil, S.J. and Ginsberg, M.H. (1996) J. Biol. Chem. 271, 6571–6574.
[19] MacKenzie, K.R. and Engelman, D.M. (1998) Proc. Natl. Acad. Sci. USA 95, 3583–3590.
[20] MacKenzie, K.R., Prestegard, J.H. and Engelman, D.M. (1997) Science 276, 131–133.
[21] Gottschalk, K.E., Adams, P.D., Brunger, A.T. and Kessler, H. (2002) Protein Sci. 11, 1800–1812.